HAL open science

2D-LWR in large-scale network with space dependent fundamental diagram

Stéphane Mollier, Maria Laura Delle Monache, Carlos Canudas de Wit

To cite this version:

Stéphane Mollier, Maria Laura Delle Monache, Carlos Canudas de Wit. 2D-LWR in large-scale network with space dependent fundamental diagram. ITSC 2018 - 21st IEEE International Conference on Intelligent Transportation Systems, Nov 2018, Maui, United States. pp.1-8. hal-01866959

HAL Id: hal-01866959

https://hal.science/hal-01866959

Submitted on 3 Sep 2018

HAL is a multi-disciplinary open access archive for the deposit and dissemination of scientific research documents, whether they are published or not. The documents may come from teaching and research institutions in France or abroad, or from public or private research centers.

L'archive ouverte pluridisciplinaire **HAL**, est destinée au dépôt et à la diffusion de documents scientifiques de niveau recherche, publiés ou non, émanant des établissements d'enseignement et de recherche français ou étrangers, des laboratoires publics ou privés.

2D-LWR in large-scale network with space dependent fundamental diagram

*

Stephane Mollier [†a], Maria Laura Delle Monache [‡b], and Carlos Canudas-de-Wit [§a]

[a]Univ. Grenoble Alpes, CNRS, Inria, Grenoble INP, GIPSA-Lab
[b]Univ. Grenoble Alpes, Inria, CNRS, Grenoble INP, GIPSA-Lab

Abstract

Traffic modeling of large-scale urban networks is a challenging task. In the literature, the network is mainly assumed to be homogeneous. However, in a large-scale scenario, it is unlikely that the traffic network characteristics–such as speed limit, number of lanes, or the network geometry–remain constant throughout the network. Therefore, we introduce a two dimensional macroscopic model for large-scale traffic networks where the fundamental diagram is space-dependent and varies with respect to the area considered. We simulate our model and compare the results with those obtained by microsimulation.
***Keywords*: Macroscopic model, space dependent flux function, large scale traffic modelling.**

1 Introduction

Macroscopic models represent traffic states with average quantities such as the density ρ, the number of vehicles per space interval, or the average velocity v. In the thirties, Greenshield [1] studied traffic with empirical observations at a specific location on the road, introducing a relation between the speed and density of vehicles. This relation is called Fundamental Diagram (FD) and is still commonly used nowadays. Twenty years later, Lighthill, Whitham [2] and then Richards [3] suggested a macroscopic model (LWR) which describes dynamically the traffic evolution. A discrete and easy to implement version, the Cell Transmission Model (CTM) is introduced in [4]. This model performs well for traffic modeling on a homogeneous road and has been validated on highway [5]. However, even on a highway the road might be variant and parameters such as the number of lanes or the speed limits may change. In these situations, the flux function does not depend only on traffic density but might also depend on space, [6], [7].

The need to model traffic in large scale urban area appears with the development of urban areas. First developed models (see [8] for the first one and [9] for a review) are two dimensional continuum static models. Then, in order to build a dynamical model for large urban areas, researchers investigate the extension of the LWR on network using models of junctions to give a representation of the intersections ([10], [11]). These models are difficult to use in practice due to the big number of parameters to calibrate. Furthermore, these models focus on a level of details which might be not relevant for the study of large scale networks. To meet the need of large scale modeling, Geroliminis and Daganzo ([12], [13]) investigate and show the existence of a Macroscopic Fundamental Diagram (MFD) which links the average flow produced in an area with the average density on that area. Thanks to this finding, accumulation models which describe the evolution of the accumulation of vehicles in a zone (called reservoir) with an Ordinary Differential Equation (ODE) can be introduced. These kinds of models keep only few information regarding the spatial distribution of vehicles, and it might not be consistent if the traffic inflow changes fast.

Finally, traffic in urban areas may be modeled with two-dimensional continuous and dynamic models. A review of some of these models is done in [14]. These models represent the traffic density ρ as a variable over a 2D-plane $(x, y) \in \Omega$. Such models are based on two-dimensional conservation law and take the following general structure:

$$\begin{cases} \dfrac{\partial \rho(t,x,y)}{\partial t} + \nabla \cdot \vec{\Phi}(\rho(t,x,y)) = 0, & \forall t \in \mathbb{R}^+, \\ \rho(0,x,y) = \rho_0(x,y), & \forall (x,y) \in \mathbb{R}^2 \end{cases} \tag{1}$$

where ρ is the aggregated density and $\vec{\Phi}$ the flow vector defined as the product of the density ρ and velocity field

*This project has received funding from the European Research Council (ERC) under the European Unions Horizon 2020 research and innovation programme (grant agreement 694209).

†stephane.mollier@gipsa-lab.fr
‡ml.dellemonache@inria.fr
§carlos.canudas-de-wit@gipsa-lab.fr

vector $\vec{v}$. This kind of two dimensional conservation law is identically considered for macroscopic modeling of pedestrians [15], [16], [17]. With the idea that for large scale modelling, a dense enough road network might be considered as a continuum, studies on two dimensional modelling for traffic is developed [18], [19], [20], [21], [22], [23]. Contrary to crowds which evolve in general in a open space, traffic flow is in general on a physical network. However, only few of the works on two dimensional models use the network geometry to parametrize their model. In [24], a flux direction per zone is defined using microsimulation on the network. In [23] and [25], the estimation of a continuous flux direction field is suggested. In [26], [27] authors considers a maximum speed that may depend on space, but these parameters are postulated instead of being extracted from the network. Furthermore, a maximum density that depends on space has not been included into the previous studies.

The contribution of this paper is to introduce a two dimensional model with space dependent flux and to suggest methods for the estimation of the model parameters which characterize the space dependency. The organization of the paper is as follows. In Section 2, the model is introduced. Then in Section 3, the estimation of space dependent parameters are described. Finally in Section 4, the numerical method is presented and the results of simulations are compared with a microsimulator (Aimsun).

2 Model construction

2.1 1D LWR with space dependent flux function

The first macroscopic models for traffic developed by Lighthill, Whitham and independently Richards (LWR models) are inspired from fluid dynamic model. These models are based on the conservation of mass and are described by a partial differential equation. In the classical LWR model in one dimension, the flux function Φ depends only on the density ρ with a relation given by the fundamental diagram (FD). An extension of this model considers a flux function that depends also on space:

$$\begin{cases} \dfrac{\partial \rho(t,x)}{\partial t} + \dfrac{\partial \Phi(x,\rho(t,x))}{\partial x} = 0, & (t,x) \in \mathbb{R}^+ \times \mathbb{R} \\ \rho(0,x) = \rho_0(x). & x \in \mathbb{R} \end{cases} \tag{2}$$

A space dependent flux might represent the variation of the speed limit along the road or a change of the number of lanes which involve a change of the maximum density. This results to a fundamental diagram that may change along the road modeled. An example of parameter variations for the fundamental diagram is shown in Figure 1.

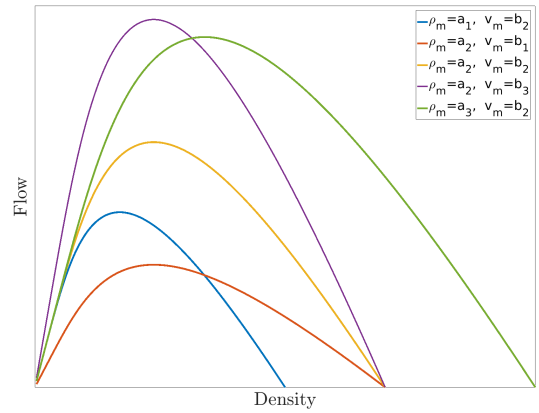

Figure 1: Variations of the parameters of the FD

This new definition of the flux function Φ involves a new formulation of the Riemann problem as it have been fully studied in [7].

$$\begin{cases} \dfrac{\partial \rho}{\partial t} + \dfrac{\partial \Phi_l(x,\rho)}{\partial x} = 0, & \rho(0,x) = \rho_l, \quad x < 0 \\ \dfrac{\partial \rho}{\partial t} + \dfrac{\partial \Phi_r(x,\rho)}{\partial x} = 0, & \rho(0,x) = \rho_r, \quad x > 0 \end{cases} \tag{3}$$

where Φ_l and Φ_r are two expressions for the flux function, respectively in the left and in right part of the domain, and ρ_l and ρ_r are the given initial conditions for the density. The solution of this problem has several new features such as the creation of stationary waves. An example of these solutions with this kind of waves is given in Figure 2.

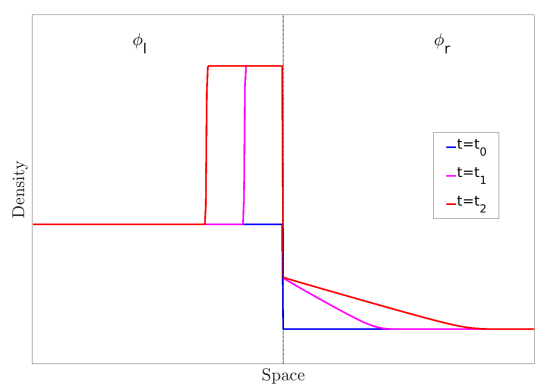

Figure 2: Solution of the Riemann problem described in (3) at different times

At the position of the flux discontinuity, we can see a stationary wave. On the left side, there is a shock wave moving backward whereas on the right side, we see a rarefaction wave. The numerical simulation in Figure 2 is done with the same demand-supply formulation that the one given in Section 4.1 and give the theoretical result expected in [7].

2.2 Description of 2D LWR model

In this section, we suggest an extension of the model introduced in [23], [25] including a space dependent flux function. This extension is even more relevant than in the one dimensional case for at least two reasons:

- As a large scale network is considered, the hypothesis that the traffic parameters (maximum density and speed limit) for all these roads are identical does not hold.
- In a two-dimensional representation of traffic, the maximum density not only depends on the number of lanes but can also depend on the concentration of roads in a specific area.

The following model is considered:

$$\begin{cases} \dfrac{\partial \rho}{\partial t}(t,x,y) + \nabla \cdot \vec{\Phi}(x,y,\rho) = 0, & \forall t \in \mathbb{R}^+, \\ \rho(0,x,y) = \rho_0(x,y). & \forall (x,y) \in \mathbb{R}^2 \end{cases} \tag{4}$$

where the flux function can be expressed as the product between velocity and density:

$$\vec{\Phi}(x,y,\rho) = \rho \ \cdot \ \vec{v}(x,y,\rho) \tag{5}$$

and the velocity field $\vec{v}(x,y,\rho)$ is given by

$$\vec{v}(x,y,\rho) = \underbrace{v(x,y,\rho)}_{\text{magnitude}} \ \cdot \ \underbrace{\vec{d}_\theta(x,y)}_{direction}, \tag{6}$$

with $v(x,y,\rho) : \mathbb{R}^2 \times [0, \rho_{\mathrm{m}}(x,y)] \to [0, v_{\mathrm{m}}(x,y)]$. ρ_{m} and v_{m} denote respectively the maximum density and maximum speed. The magnitude is given by a space dependent fundamental diagram:

$$v(x,y,\rho) = v_{\mathrm{m}}(x,y)\left(1 - \exp\left(\alpha\left(1 - \frac{\rho_{\mathrm{m}}(x,y)}{\rho}\right)\right)\right) \tag{7}$$

The parameter α is chosen constant equal to 0.4 such that the ratio between the critical density ρ_{c} and the maximum density ρ_{m} remains constant. The shape of the fundamental diagram at a given space position (x,y) can be seen in Figure 3.

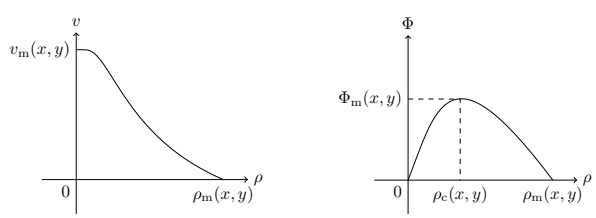

(a) Relation velocity density

(b) Relation flux density: FD

Figure 3: Speed and flow vs. density.

The definition and estimation of $\vec{d}_\theta$, v_{m} and ρ_{m} will be respectively presented in the Section 3.2, 3.3 and 3.4.

3 Network considered and parameters estimation

3.1 Study case

For simulation and test purposes, the network considered is a 10×10 or 1km square Manhattan grid with the position of the nodes slightly distorted with a white noise (of standard deviation 30m) in order to have a less regular network. We assume that all the roads considered are one way and globally oriented towards the North-East direction. As we are interested in studying the space dependency of the flux function, we consider an area in the middle of the network with low concentration of roads such that the maximum density in this zone is lower. This could represent a physical bottleneck for people willing to go from West to East. Furthermore, we set the speed limits on all road equal to 30 km/h (which is reasonable for roads in the city center) except for one main arterial set to 50km/h such that the maximum speed over the network is not constant. This network is represented in Figure 4.

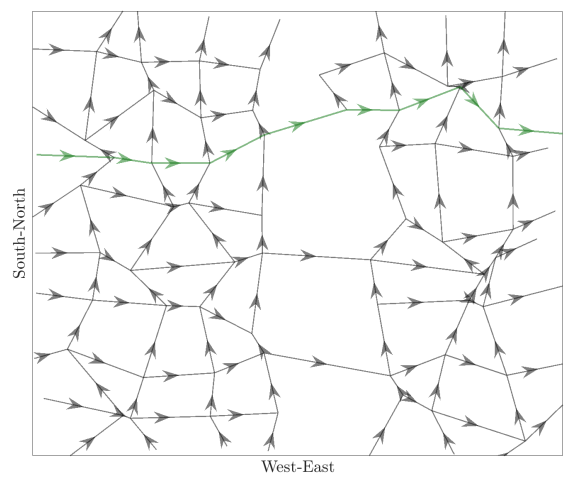

Figure 4: Network considered for simulation. The main arterial is represented in green.

3.2 Velocity direction field

In this section, we recall the estimation method introduced in [23], [25]. We denote by $q \in \{1, .., Q\}$ the different roads of the network. The spatial path of each road is described by a parametric curve $\Psi^q : s \in [0, s_{\max}] \to (\Psi_1^q(s), \Psi_2^q(s)) \in \mathbb{R}^2$. The variable $s \in [0, s_{\max}]$ allows to progress along the road curvature from an intersection to the next one. Let $\vec{\tau^q}(\Psi^q(s))$ be the unit tangent vector of the road q at position $(\Psi_1^q(s), \Psi_2^q(s))$.

The estimation of the unit vector $\vec{d}_\theta$ is done by a spatial

interpolation method called Inverse Distance Weighting:

$$\vec{d_\theta}(x,y) = \frac{\sum_{q=1}^{Q} \int_{s\in[0,s_{\max}]} w(l(x,y,s))\vec{\tau^q}(\Psi^q(s))ds}{\left|\left|\sum_{q=1}^{Q} \int_{s\in[0,s_{\max}]} w(l(x,y,s))\ \vec{\tau^q}(\Psi^q(s))ds\right|\right|} \quad (8)$$

where $l : (x,y,s) \to \|(x,y) - (\Psi^q(s))\|$ is the distance from the point (x,y) to the road. The weight function $w : \mathbb{R}^+ \to \mathbb{R}^+$ should be a decreasing function of the distance.

$$w : X \to e^{-\beta X} \qquad \text{with} \qquad \beta > 0,$$

the parameter β represents the sensitivity of the function to the distance.

For the considered network, the velocity field is estimated with a parameter β equal to 20. An estimation of the velocity field with a larger mesh can be seen in Figure 5.

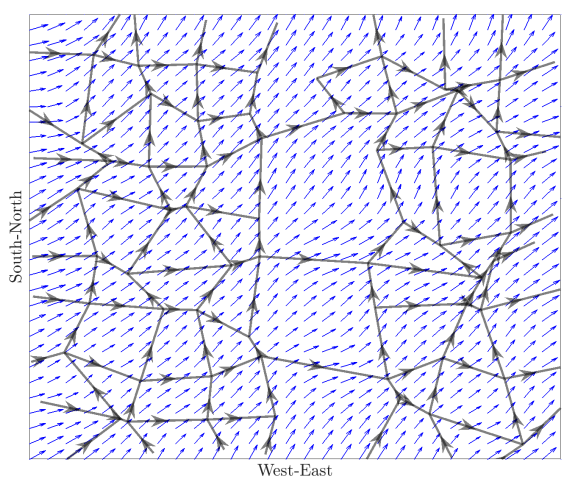

Figure 5: Interpolation of velocity field $\vec{d_\theta}(x,y)$ using the network geometry

3.3 Reconstruction of a two dimensional density from individual vehicles and estimation of space dependent maximum density

In this section, we recall a method to reconstruct a two dimensional density from the observation of individual vehicles on the spirit of [25] using the Kernel Density Estimation (KDE) method. The idea is that each individual vehicle have a contribution to the global density estimation with a Gaussian kernel centered in the vehicle position. Let $(x_k^n, y_k^n)_{k\in[1\cdot K(n)]}$ be the position of vehicles within the network at time t^n. Then we can reconstruct the density at this time over the network as follows:

$$\tilde{\rho}^n(x,y) = \sum_{k=1}^{K(n)} G_{2d}\left(\begin{pmatrix} x \\ y \end{pmatrix} - \begin{pmatrix} x_k^n \\ y_k^n \end{pmatrix}\right) \quad (9)$$

with

$$G_{2d}(x,y) = \frac{e^{-\frac{x^2+y^2}{2d_0^2}}}{2\pi d_0^2} \text{ s.t. } \iint_{\mathbb{R}^2} G_{2d}(x,y)\ dx\ dy = 1,$$

d_0 is a parameters that control the range of the Gaussian function. We set d_0 equal to 50m. This method allows to reconstruct a two dimensional density either from real data (GPS probes) or from a microsimulator (for instance Aimsun).

With these notions, we are now able to describe the method to estimate the space dependent maximum density $\rho_{\mathrm{m}} : \Omega \to \mathbb{R}_+$. Let us now consider that we have a fully congested network. We set the headway between two consecutive vehicles equal to 6m which is a rough estimate of the value obtained from real traffic data in urban area [13]. Then, we assume that in every road and each 6m there is a vehicle. We denote by $(x_k, y_k)_{k\in\{1,\cdots,K_{\max}\}}$ the position of all these vehicles. Thus, we estimate the maximal density of the network as follows:

$$\rho_{\mathrm{m}}(x,y) = \sum_{k=1}^{K_{\max}} G_{2d}\left(\begin{pmatrix} x \\ y \end{pmatrix} - \begin{pmatrix} x_k \\ y_k \end{pmatrix}\right). \quad (10)$$

The estimated maximum density obtained with this method can be shown in Figure 6. For the color scale

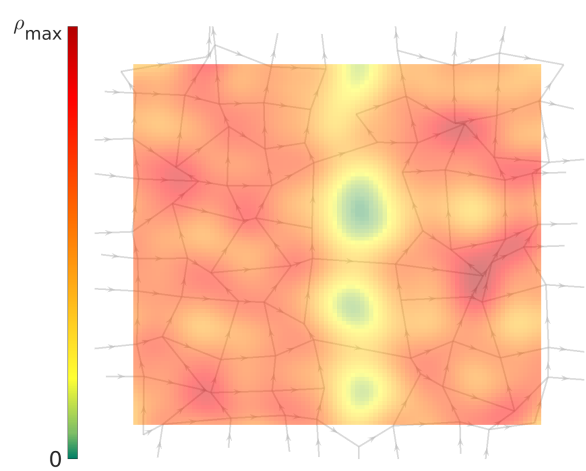

Figure 6: Estimation of the maximum density $\rho_{\mathrm{m}}(x,y)$ over the 2D-plane using the proposed method for a parameter d_0 set to 50m

to represent the density, we define:

$$\rho_{\max} = \max_{(x,y)\in\mathbb{R}^2} \rho_{\mathrm{m}}(x,y). \quad (11)$$

We can notice that in the central area of the network, a lower concentration of roads involves a lower estimation of the maximum density. To avoid issue on the reconstruction near the boundary, we considered an extension of the network just for the estimation of the maximum density (see Figure 6 in comparison with Figure 4).

3.4 Reconstruction of space dependent maximum speed

For the estimation of the maximum speed, we use an interpolation method as in Section 3.2. We keep the same notation with $q \in \{1, \cdots, Q\}$ the different roads and $\Psi^q : s \in [0, s_{\max}] \to (\Psi_1^q(s), \Psi_2^q(s)) \in \mathbb{R}^2$ the parametric curves that describes the paths of each road. Let $v^q(\Psi^q(s))$ be the speed limit of the road q at position $(\Psi_1^q(s), \Psi_2^q(s))$. The estimation of maximum velocity over the 2D-plane v_{m} is done by the spatial interpolation method:

$$v_{\mathrm{m}}(x,y) = \frac{\sum_{q=1}^{Q} \int_{s\in[0,s_{\max}]} w(l(x,y,s)) v^q(\Psi^q(s)) ds}{\left\| \sum_{q=1}^{Q} \int_{s\in[0,s_{\max}]} w(l(x,y,s)) ds \right\|} \tag{12}$$

where $l : (x,y,s) \to \|(x,y) - (\Psi^q(s))\|$ is the distance from the point (x,y) to the road and where

$$w : X \to e^{-\beta X} \qquad \text{with} \qquad \beta > 0.$$

The estimated maximum velocity field can be seen in Figure 7. A path with a higher maximum speed is

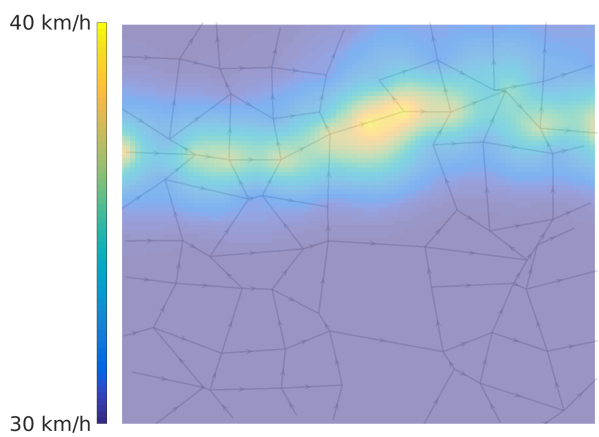

Figure 7: Interpolation of the maximum speed $v_{\mathrm{m}}(x,y)$ from the speed limit of the roads

described along the arterial road as expected. For the interpolation of the maximum speed v_{m}, an important remark is that the estimation does not depend on the road concentration but only on the the value of the speed limit of the neighbouring roads.

4 Simulation results

4.1 Numerical method

Numerical methods for conservation laws are well studied in the literature [7], [28], [29]. Here, an extrapolation of the well know Cell Transmission Model (CTM) [4] which includes space dependency of the flux is considered. Then, the two dimensional aspect is considered by using dimensional splitting. Let $(C_{i,j})_{(i,j)\in[1..I]\times[1..J]}$ be the cell space discretization and (x_i, y_j) be the coordinates of each cell center. Applying the method given in section 3.2, we can define a flux direction for each cell

$$\vec{d_\theta}(x_i, y_j) = \begin{cases} \cos(\theta_{i,j}) \\ \sin(\theta_{i,j}) \end{cases} \tag{13}$$

Let us define the density in the cells with $(\rho_{i,j})_{(i,j)\in[1..I]\times[1..J]}$, then the numerical flux is defined at cell interfaces with the notation $F_{i+\frac{1}{2},j} = F(\rho_{i,j}, \rho_{i+1,j})$ and the function F is defined as follows:

$$F_{i+\frac{1}{2},j} = \begin{cases} \min(D_{i,j}, S_{i+1,j}) \text{ if } \cos(\theta_{i+\frac{1}{2},j}) \geq 0 \\ \min(S_{i,j}, D_{i+1,j}) \text{ if } \cos(\theta_{i+\frac{1}{2},j}) < 0 \end{cases} \tag{14}$$

Here $\theta_{\mathrm{i,j}}$ is the angle (see (13)) of the unit vector direction of the flux $\vec{d_\theta}(x_{\mathrm{i}}, y_{\mathrm{j}})$ defined in Section 3.2 at cell $C_{i,j}$, and $\cos(\theta_{\mathrm{i}+\frac{1}{2},\mathrm{j}})$ is defined equal to $\frac{\cos(\theta_{\mathrm{i}+1,\mathrm{j}})+\cos(\theta_{\mathrm{i,j}})}{2}$. $D_{i,j}$ and $S_{i,j}$ are respectively the demand and supply function of the cell $C_{i,j}$ which could be defined as follows:

$$D_{i,j} = \begin{cases} \Phi(x_i, y_j, \rho_{i,j}), & \text{if } \rho_{i,j} \leq \rho_{\mathrm{c}}(x_i, y_j) \\ \Phi_{\mathrm{m}}(x_i, y_j), & \text{if } \rho_{i,j} > \rho_{\mathrm{c}}(x_i, y_j) \end{cases} \tag{15}$$

$$S_{i,j} = \begin{cases} \Phi_{\mathrm{m}}(x_i, y_j), & \text{if } \rho_{i,j} \leq \rho_{\mathrm{c}}(x_i, y_j) \\ \Phi(x_i, y_j, \rho_{i,j}), & \text{if } \rho_{i,j} > \rho_{\mathrm{c}}(x_i, y_j) \end{cases} \tag{16}$$

with the flux $\Phi(x_i, y_j, \rho_{i,j}) = \rho_{i,j} \cdot v(x_i, y_j, \rho_{i,j})$ and his maximum $\Phi_{\mathrm{m}}(x_i, y_j) = \rho_{\mathrm{c}}(x_i, y_j) \cdot v(x_i, y_j, \rho_{\mathrm{crit}}(x_i, y_j))$. The velocity function v is the one defined in Section 2.2 with the parameters ρ_{m} and v_{m} estimated respectively in Section 3.3 and 3.4. $\rho_{\mathrm{c}}(x_i, y_j)$ is the corresponding critical density for a maximum density $\rho_{\mathrm{m}}(x_i, y_j)$. The vertical flux $F_{i,j+\frac{1}{2}}$ is defined analogously.

Let Δt be the time step, and Δx and Δy the space discretization with respect to the x-axis and the y-axis. Then the global scheme for the computation of the model can be defined with the dimensional splitting as follows:

$$\rho^*_{\mathrm{i,j}} = \rho^{\mathrm{n}}_{\mathrm{i,j}} - \frac{\Delta t}{\Delta x}\Big(\cos(\theta_{\mathrm{i}+\frac{1}{2},\mathrm{j}}) F^n_{\mathrm{i}+\frac{1}{2},\mathrm{j}} - \cos(\theta_{\mathrm{i}-\frac{1}{2},\mathrm{j}}) F^n_{\mathrm{i}-\frac{1}{2},\mathrm{j}} \Big), \tag{17}$$

$$\rho^{n+1}_{\mathrm{i,j}} = \rho^*_{\mathrm{i,j}} - \frac{\Delta t}{\Delta y}\Big(\sin(\theta_{\mathrm{i,j}+\frac{1}{2}}) F^*_{\mathrm{i,j}+\frac{1}{2}} - \sin(\theta_{\mathrm{i,j}-\frac{1}{2}}) F^*_{\mathrm{i,j}-\frac{1}{2}} \Big), \tag{18}$$

where the variables are:

- $\rho^{\mathrm{n}}_{\mathrm{i,j}}$, $\rho^{\mathrm{n+1}}_{\mathrm{i,j}}$ are the discrete density at time t^n and t^{n+1}

- $\rho^*_{\mathrm{i,j}}$ is an intermediate value used only for computation
- Δx, Δy, Δt are space and time step discretization
- $F^n_{\mathrm{i}+\frac{1}{2},\mathrm{j}}$ is the flux at the cell interface
- $\cos(\theta_{\mathrm{i}+\frac{1}{2},\mathrm{j}})$ and $\sin(\theta_{\mathrm{i},\mathrm{j}+\frac{1}{2}})$ are the contribution of the flow direction.

4.2 Simulation results

The validation of the model is done by comparing the model prediction and the one given by the microsimulator Aimsun. To this aim, a simulation for the same network and scenario is run for the two. In order to be able to compare these results, a two-dimensional density is reconstructed from the vehicles' trajectories of the Aimsun simulation using the method described in Section 3.3.

4.2.1 Scenario description

The scenario considered represents a dissipation of a congestion. In the microsimulator, an important concentration of vehicles is artificially generated in the South-East of the network and set as an initial condition for the simulation. The split ratio at each intersection is equal to 50 % except for the roads across the bottleneck of the network where vehicles have 70 % split ratio. With the method described in Section 3.3 and also in [25], a two-dimensional density is reconstructed and given as initial condition of the 2D model. Then, the two models are run independently assuming that there is no inflows in both cases. The 2D model provides a propagation of density whereas the microsimulator describes the evolution of each vehicle's trajectory. At each time step (which has been synchronized), the results of the models can be compared by reconstructing a 2D density from the vehicles' position of the Aimsun Simulation. The network characteristics defined for the microsimulator are identical to those considered for the estimation of the model parameters. Thus, the minimum headway between vehicles is set to 6m and the road speed limits are set equal to 30 or 50km/h.

4.2.2 Results of the comparison with the microsimulator

We simulate the scenario described above. The comparison between the results of the two models can be seen in Figure 8. A first remark is that in the microsimulator the congestion does not propagate across the bottleneck and remain in the left side of the network. This phenomena is also captured by the two-dimensional model where a discontinuity in the density appears next to the network bottleneck. It is a stationary wave, a classical feature that can be seen when considering space dependent flux function. Another remark is that we choose to show the comparison with absolute value of the density where the scale is given by the maximum over the space of the maximum density. This choice could give an impression that the network is only slightly congested. Another possibility might be to represent the relative density with respect to the maximum density estimated

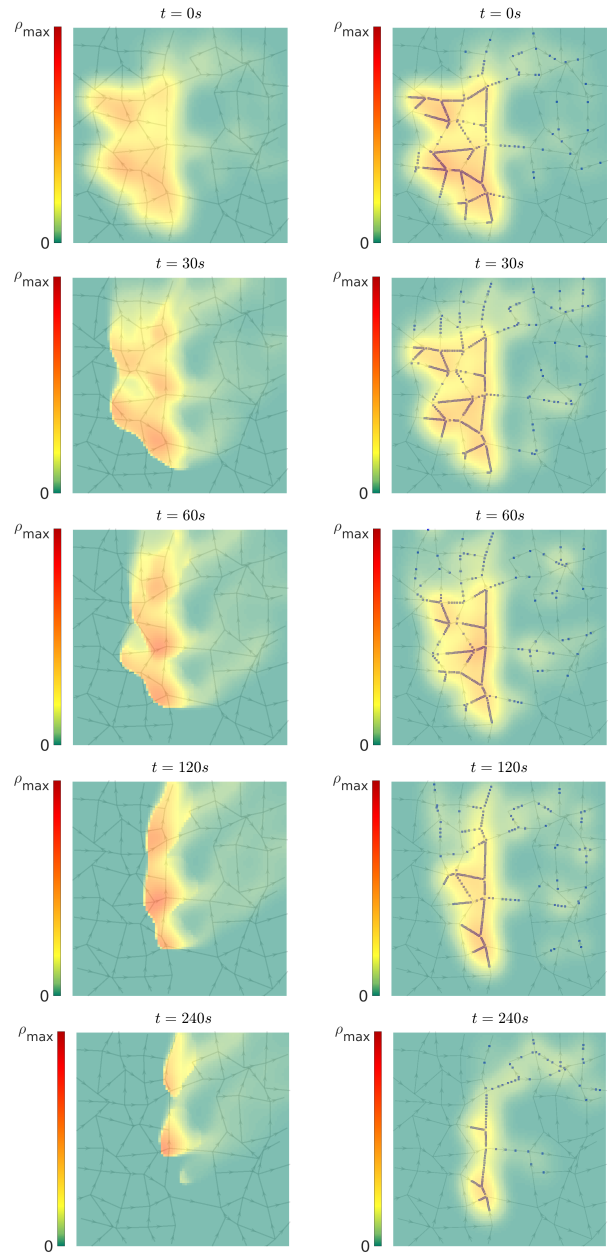

Figure 8: Comparison between the 2D model with space dependent flux function (left) and the 2D density reconstructed from the microsimulator (right) for a scenario of congestion dissipation. The blue squares represent vehicles of the microsimulation. A video of the simulation is available on https://youtu.be/qWNnnpFJZeQ.

on each space position. However, it might be difficult to interpret the motion and location of the vehicles within the network.

Conclusion

This paper investigated the extension of a two dimensional model with space dependency in the flux function, i.e. with a varying fundamental diagram. A methodology for the estimation of the main parameters such as the maximum density and the free flow speed were suggested. Results of the model were compared with the results of the microsimulator Aimsun.

Acknowledgements

This project has received funding from the European Research Council (ERC) under the European Unions Horizon 2020 research and innovation programme (grant agreement 694209).

References

[1] B. D. Greenshields, J. Thompson, H. Dickinson, and R. Swinton, "The photographic method of studying traffic behavior," in *Highway Research Board Proceedings*, vol. 13, 1934.

[2] M. J. Lighthill and G. B. Whitham, "On kinematic waves. ii. a theory of traffic flow on long crowded roads," in *Proceedings of the Royal Society of London A: Mathematical, Physical and Engineering Sciences*, vol. 229, pp. 317–345, The Royal Society, 1955.

[3] P. I. Richards, "Shock waves on the highway," *Operations research*, vol. 4, no. 1, pp. 42–51, 1956.

[4] C. F. Daganzo, "The cell transmission model: A dynamic representation of highway traffic consistent with the hydrodynamic theory," *Transportation Research Part B: Methodological*, vol. 28, no. 4, pp. 269–287, 1994.

[5] A. Kotsialos, M. Papageorgiou, C. Diakaki, Y. Pavlis, and F. Middelham, "Traffic flow modeling of large-scale motorway networks using the macroscopic modeling tool metanet," *IEEE Transactions on intelligent transportation systems*, vol. 3, no. 4, pp. 282–292, 2002.

[6] R. Bürger and K. H. Karlsen, "Conservation laws with discontinuous flux: a short introduction," *Journal of Engineering Mathematics*, vol. 60, no. 3-4, pp. 241–247, 2008.

[7] H. Holden and N. H. Risebro, *Front tracking for hyperbolic conservation laws*, vol. 152. Springer, 2015.

[8] M. Beckmann, "A continuous model of transportation," *Econometrica: Journal of the Econometric Society*, pp. 643–660, 1952.

[9] H. Ho and S. Wong, "Two-dimensional continuum modeling approach to transportation problems," *Journal of Transportation Systems Engineering and Information Technology*, vol. 6, no. 6, pp. 53–68, 2006.

[10] G. M. Coclite, M. Garavello, and B. Piccoli, "Traffic flow on a road network," *SIAM journal on mathematical analysis*, vol. 36, no. 6, pp. 1862–1886, 2005.

[11] M. Garavello, K. Han, and B. Piccoli, *Models for vehicular traffic on networks*, vol. 9. American Institute of Mathematical Sciences (AIMS), Springfield, MO, 2016.

[12] C. F. Daganzo and N. Geroliminis, "An analytical approximation for the macroscopic fundamental diagram of urban traffic," *Transportation Research Part B: Methodological*, vol. 42, no. 9, pp. 771–781, 2008.

[13] N. Geroliminis and C. F. Daganzo, "Existence of urban-scale macroscopic fundamental diagrams: Some experimental findings," *Transportation Research Part B: Methodological*, vol. 42, no. 9, pp. 759–770, 2008.

[14] R. Aghamohammadi and J. A. Laval, "Dynamic traffic assignment using the macroscopic fundamental diagram: A review of vehicular and pedestrian flow models," *arXiv preprint arXiv:1801.02130*, 2018.

[15] D. Helbing, "A fluid dynamic model for the movement of pedestrians," *arXiv preprint cond-mat/9805213*, 1998.

[16] R. L. Hughes, "A continuum theory for the flow of pedestrians," *Transportation Research Part B: Methodological*, vol. 36, no. 6, pp. 507–535, 2002.

[17] Y.-q. Jiang, P. Zhang, S. Wong, and R.-x. Liu, "A higher-order macroscopic model for pedestrian flows," *Physica A: Statistical Mechanics and its Applications*, vol. 389, no. 21, pp. 4623–4635, 2010.

[18] Y. Jiang, S. Wong, H. Ho, P. Zhang, R. Liu, and A. Sumalee, "A dynamic traffic assignment model for a continuum transportation system," *Transportation Research Part B: Methodological*, vol. 45, no. 2, pp. 343–363, 2011.

[19] J. Du, S. Wong, C.-W. Shu, T. Xiong, M. Zhang, and K. Choi, "Revisiting jiang's dynamic continuum model for urban cities," *Transportation Research Part B: Methodological*, vol. 56, pp. 96–119, 2013.

[20] L. Romero Perez and F. G. Benitez, "Outline of diffusion advection in traffic flow modeling," in *Transportation Research Board 87th Annual Meeting*, no. 08-1503, 2008.

[21] T. Saumtally, *Modèles bidimensionnels de trafic*. PhD thesis, Université Paris-Est, 2012.

[22] M. Herty, A. Fazekas, and G. Visconti, "A two-dimensional data-driven model for traffic flow on highways," 2017.

[23] S. Mollier, M. L. Delle Monache, and C. Canudas-de Wit, "A simple example of two dimensional model for traffic: discussion about assumptions and numerical methods," *Transportation Research Record (TRR), Journal of the Transportation Research Board*, 2018. https://hal.archives-ouvertes.fr/hal-01665285.

[24] F. Della Rossa, C. D'Angelo, and A. Quarteroni, "A distributed model of traffic flows on extended regions.," *NHM*, vol. 5, no. 3, pp. 525–544, 2010.

[25] S. Mollier, M. L. Delle Monache, C. Canudas-de Wit, and B. Seibold, "Two-dimensional macroscopic model for large scale traffic networks." Preprint https://hal.archives-ouvertes.fr/hal-01819013, 2018.

[26] Y.-Q. Jiang, P.-J. Ma, and S.-G. Zhou, "Macroscopic modeling approach to estimate traffic-related emissions in urban areas," *Transportation Research Part D: Transport and Environment*, 2015.

[27] Z. Lin, S. Wong, P. Zhang, Y. Jiang, K. Choi, and Y. Du, "A predictive continuum dynamic user-optimal model for a polycentric urban city," *Transportmetrica B: Transport Dynamics*, vol. 5, no. 3, pp. 228–247, 2017.

[28] E. F. Toro, *Riemann solvers and numerical methods for fluid dynamics: a practical introduction*. Springer Science & Business Media, 2013.

[29] K.-A. Lie, "A dimensional splitting method for quasilinear hyperbolic equations with variable coefficients," *BIT Numerical Mathematics*, vol. 39, no. 4, pp. 683–700, 1999.